

## Heavy Metals and Radionuclides Sorption and Removal from Ground Water by Graphene Oxide (GO) and its Derivatives

*Khaled M. Naguib*

Sanitary and Environmental Engineering Institute,  
Housing and Building National Research Center, Egypt

---

**Abstract:** This research shows the efficiency of graphene oxide (GO) for rapid removal of some of the most toxic and radioactive long-lived human-made radionuclides from contaminated water, even from acidic solutions (pH < 2). The interaction of GO with actinides including Am(III), Th(IV), Pu(IV), Np(V), U(VI) and typical fission products Sr(II), Eu(III) and Tc(VII) were studied, along with their sorption kinetics. Cation/GO coagulation occurs with the formation of nanoparticle aggregates of GO sheets, facilitating their removal. In the presented work, new composite nanomaterials, based on graphene oxide and styrene, have been developed for the retention purpose. <sup>85</sup>Sr and <sup>137</sup>Cs represent two of the main fission products being present in radioactive wastes from nuclear power cycle. The graphene oxide samples were prepared from natural graphite using high intensity cavitation field in a pressurized (6 bar) batch-ultrasonic reactor. Graphene oxide (GO) and two magnetic graphene oxide (MGO) composites with a different amount of magnetite were synthesized, characterized and used in sorption experiments. The effect of pH on sorption of Am(III) and Pu(IV) isotopes as well as Co(II), Ni(II), Cu(II) and Pb(II) to GO and MGO was studied in equilibrium and kinetic experiments. The adsorption capacities varied from 30 to 574 mg g<sup>-1</sup> while rate constants ranged from 0.29 to 0.46 min<sup>-1</sup> and increased in the following order Co, Cu, Pb and Ni. Large variations in the uptake of studied elements by adsorbents depending on initial and final pH of solutions were observed.

**Key words:** Graphene oxide • Sorption • Radionuclide • Heavy metals.

---

### INTRODUCTION

Naturally occurring radioactive materials (NORM) are abundant throughout the earth's crust. Human manipulation of NORM for economic ends, such as mining, ore processing, fossil fuel extraction and commercial aviation, may lead to what is known as "technologically enhanced naturally occurring radioactive materials" (TENORM). The existence of TENORM results in an increased risk for human exposure to radioactivity. TENORM-producing industries may cause workers to be occupationally exposed to ionizing radiation and may release significant amounts of radioactive material into the environment resulting in the potential for widespread exposure. These industries include mining, phosphate processing, metal ore processing, heavy mineral sand processing, titanium pigment production, fossil fuel extraction and combustion, manufacture of building materials, thorium compounds, aviation and scrap metal processing [1].

Treatment and decontamination of waste products and two-dimensional honeycomb network [2].

An advance in graphite-related materials promises to finally mitigate a long-standing problem for the resource development industries. Graphene oxide (GO), which is non-conductive, hydrophilic and easily suspended in water is able to clean radionuclide-contaminated liquids by agglomerating contaminants into solids.

There are realistically three strategies for ensuring that contaminated groundwater containing human-made radionuclides, among which the transuranic elements are the most toxic, is an essential task in the clean-up of legacy nuclear sites [3]. The recent accident that included radionuclide release to the environment at the Fukushima Daiichi nuclear power plant in Japan and the contamination of the water used for cooling its reactor cores, underscores the need for effective treatment methods of radionuclide-contaminated water [4].

---

**Corresponding Author:** Khaled M. Naguib, Sanitary and Environmental Engineering Institute,  
Housing and Building National Research Center, Egypt.

Graphene and related materials such as GO, reduced GO and various nanocomposites have attracted great attention since the graphene discovery in 2004 [5]. Their unique properties and a wide range of physical and engineering applications in various fields as well as their high potential for the efficient removal of various pollutants including the most toxic long-lived radionuclides from contaminated solutions made them the most promising materials of the twenty first century [6-8]. It is generally accepted that graphene is a flat single layer of sp<sup>2</sup> hybridized carbon atoms, densely packed into an ordered structure. Radioactive materials don't cause harm to people or the environment:

- Separation,
- Isolation,
- Transmutation, a nuclear reaction by bombarding the material with neutrons or protons from an accelerator or a reactor to form isotopes with short half-lives.

The last approach, while highly effective, is developmental and prohibitively expensive to consider for anything less radioactive than spent nuclear fuel, so the only realistic options are separation and isolation. The role that GO can play in these options is separation [9].

The invention of a GO filtration system originated through an international collaboration led by the efforts of James Tour in the Nanomaterial's Research Lab at Rice University in Houston and Stepan Kalmykov in the Environmental Radioactivity Research Lab at Moscow State University. Although it is still in a stage of development, it is being introduced in a variety of systems configurations through the efforts of VSW Water Purity, LLC, in Grapevine, Texas. In this system, GO powder is suspended in water and coagulates when heavy metal ions are introduced to the solution. It is then easily separated by sedimentation or rough mechanical filtering.

The properties of GO suspended in solution make it a promising material in rheology and colloidal chemistry [10, 11]. The hydrophilic GO produces stable suspensions when dispersed in liquids and shows excellent adsorption capacities due to its relatively vast and highly accessible surface area, lack of internal surfaces, which usually cause slow cation-sorbent interactions and its significant negative charge [12-14].

**Sample Preparation:** Preparing samples for this experiment requires that certain precautions be taken. First, all samples should be prepared in the fume hood in

order to contain any harmful fumes and or radioactive material. Lab coat, goggles and gloves taped to the sleeves of the lab coat are required as well.

In order to prepare a solution of 1 part per million (ppm) of uranium, a sample of uranium oxide (UO<sub>2</sub>) will be used. Nitric acid (HNO<sub>3</sub>) will break down the UO<sub>2</sub> and create a water soluble salt of uranyl nitrate (UO<sub>2</sub>•(NO<sub>3</sub>)<sub>2</sub>). This salt will then be dissolved in deionized water to produce a 1ppm solution of uranium. Once the sample solution has been produced, it should be stored in a glass container with a cap. The cap of the container should be taped to ensure a good seal and to prevent a possible release of radioactive material. The container should also be labeled with its contents, the date of creation and the name of person who created it. This container should then be stored in a radioactive safety locker.

Preparation of a solution containing 0.5 ppm of <sup>137</sup>Cs and 0.5 ppm of <sup>90</sup>Sr, for a total of 1 ppm concentration of radioactive elements will use a slightly different technique. Strontium nitrate (Sr•(NO<sub>3</sub>)<sub>2</sub>) and cesium nitrate (Cs•NO<sub>3</sub>) salts will be added directly to deionized water in order to create the solution. Once this has been accomplished, trace amounts of radioactive isotopes <sup>137</sup>Cs and <sup>90</sup>Sr will be added to the solution. Once the sample solution has been produced, it should be stored in a glass container with a cap. The cap of the container should be taped to ensure a good seal and to prevent a possible release of radioactive material. The container should also be labeled with its contents, the date of creation and the name of person who created it. This container should then be stored in a radioactive safety locker.

High resolution scanning electron microscopy (HRSEM) analysis was conducted on a FEI Nova Nano SEM scanning electron microscope equipped with an Everhart-Thornley detector, Through Lens detector and accelerating voltage 1-30 kV. The sample was deposited on the silicon chip substrate 5x5 mm.

Diffraction patterns were collected with diffractometer Bruker D2 equipped with conventional X-ray tube (Cu K $\alpha$  radiation, 30 kV, 10 mA). The primary divergence slit module width 0.6 mm, Soller Module 2.5, Airscatter screen module 2 mm, Ni Kbeta-filter 0.5 mm, step 0.00405°, a counting time per a step 1 s and the LYNXEYE 1-dimensional detector were used. The range of measurement is from 5° to 90° 2Theta.

Qualitative analysis was performed with the Diffrac Plus Eva software package (Bruker AXS, Germany) using the JCPDS PDF-2 database. For quantitative analysis of XRD patterns we used Diffrac-Plus Topas (Bruker AXS, Germany, version 4.1) with structural models

based on ICSD database. This program permits to estimate the weight fractions of crystalline phases and mean coherence length by means of Rietveld refinement procedure.

**Characterization:** GO and MGO were characterized by Mössbauer spectroscopy, X-ray diffraction (XRD), Fourier transform infrared spectroscopy (FTIR) and Scanning electron microscopy (SEM) (Fig. 1). The Mössbauer spectra were acquired at room temperature applying. The Mössbauer spectrometer in the transmission geometry using the  $^{57}\text{Co}(\text{Rh})$  source. NormosDist software was used for analysis of spectra. The XRD analyses were conducted by means of a D8 (Bruker AXS) X-ray diffractometer.

SEM was used to observe the surface state and structure of the samples using the scanning electron microscope (High resolution FESEM Su-70 Hitachi). FTIR spectra were obtained with the ATR-FTIR Perkin Elmer spectrophotometer using the MCD detector with a scan range of  $4000\text{--}400\text{ cm}^{-1}$ .

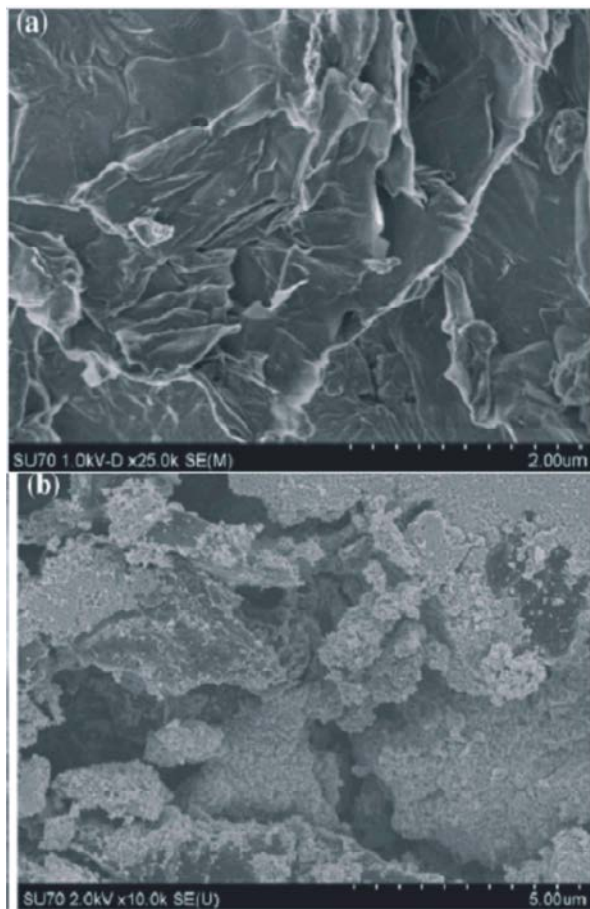


Fig. 1: SEM images of GO (a) and MGO composite (b)

**Experimental:** GO was prepared using the improved Hummer's method. Large-flake graphite (10.00 g, Sigma-Aldrich, CAS 7782-42-5, LOT 332461-2.5 KG, Batch #13802EH) was suspended in a 9 : 1 mixture of sulfuric and phosphoric acids (400 mL) and then potassium permanganate (50.00 g, 0.3159 mol) was added in small portions over a 24 h period. After 5 d the suspension was quenched with ice (1 kg) and the residual permanganate was reduced with  $\text{H}_2\text{O}_2$  (30% aqueous, ~3 mL) until the suspension became yellow. The product was isolated by centrifugation at  $319g$  for 90 min (Sorvall T1, ThermoFisher Scientific) and subsequently washed with 10% HCl and water. The yellow-brown water suspension (190.0 g) was isolated, corresponding to 10 g of dry product. For gravimetric analysis 50 mL of main product was separated from main batch, washed as described above and reduced by excess  $\text{N}_2\text{H}_4$ . It is important to note that the product isolation process produced significant amounts of contaminated organic solvents that could be considered environmentally hazardous. However, this process could be changed or omitted in an industrial procedure and is used here only to allow characterization of starting material by removal of water and manganese II–IV) oxides [15].

Sorption experiments were carried out in plastic vials for which sorption onto the vial walls was negligible under the experimental conditions. In the sorption experiments, solutions of the radionuclides nitrates (each radionuclide experiment was done separately) were added to GO suspension and then the pH was measured using a combined glass pH electrode (InLab Expert Pro, Mettler Toledo) and adjusted by addition of small amounts of dilute  $\text{HClO}_4$  or NaOH. After equilibration, the GO suspension was centrifuged at  $40\,000g$  for 20 min (Allegra 64R, Beckman Coulter) to separate radionuclides sorbed onto the GO. The sorption was calculated from the difference between the initial activity of the radionuclides and that measured in solution after equilibration. The initial total concentration of radionuclides in the kinetic experiments and pH-dependence tests was  $2.15 \times 10^{-7}\text{ M}$  for  $^{233}\text{U}(\text{VI})$ ,  $1.17 \times 10^{-9}\text{ M}$  for  $^{239}\text{Pu}(\text{IV})$ ,  $5.89 \times 10^{-14}\text{ M}$  for  $^{234}\text{Th}(\text{IV})$ ,  $3.94 \times 10^{-10}\text{ M}$  for  $^{241}\text{Am}(\text{III})$ ,  $3.43 \times 10^{-12}\text{ M}$  for  $^{152}\text{Eu}(\text{III})$ ,  $3.77 \times 10^{-7}\text{ M}$  for  $^{237}\text{Np}(\text{V})$ ,  $1.91 \times 10^{-7}\text{ M}$  for  $^{95m}\text{Tc}(\text{VII})$  and  $1.24 \times 10^{-7}\text{ M}$  for  $^{90}\text{Sr}(\text{II})$ . The concentration of the GO suspension was  $0.077\text{ g L}^{-1}$  in  $0.01\text{ M NaClO}_4$ . In all cases the total concentration of ions was much less than the solubility limit and the GO/radionuclide ratio correspond to a very high under-saturation of GO sorption sites [15].

For desorption tests, HClO<sub>4</sub> was added to the suspensions to decrease pH and after different time intervals the concentration of radionuclides in solution was measured. To measure the sorption capacity of GO towards different radionuclides, the sorption isotherms were obtained using 0.038 g L<sup>-1</sup> GO suspension in 0.01 M NaClO<sub>4</sub> in case of U(VI), Sr(II), Am(III) and 0.38 g L<sup>-1</sup> GO suspension in 0.01 M NaClO<sub>4</sub> in case of Eu(III). The concentration of the cations was varied at constant pH values [15].

XPS was performed on PHI Quantera XPS with Al source. TGA Q50 (TA Instruments) was used for TGA; B10 mg of homogenized sample was investigated. Temperature was increased at a rate of 20 °C min<sup>-1</sup> to 150 °C, held at 150 °C for 1 h and then the temperature was raised at a rate of

10 °C min<sup>-1</sup>. FTIR analysis was performed in reflection geometry using Nicolet FTIR Infrared Microscope Samples for FTIR, Raman and XPS were drop-cast onto glass substrates and dried under vacuum for 48 h to form detachable free-standing graphene oxide paper. To trace the changes that occur with GO upon interaction with cations, the sample was equilibrated with Eu(III) to prepare it for IR and XPS examinations. Experimental conditions were similar to those described for the isotherm experiments, using 0.38 g L<sup>-1</sup> GO suspension in water. Concentration of Eu was determined to be 1 mM by gravimetric analysis of source EuCl<sub>3</sub> salt (Aldrich, CAS 13759-92-7) that was dried with SOCl<sub>2</sub> and subsequently dried under vacuum [15].

To demonstrate the performance of GO compared to other sorbents for radionuclide removal, experiments were conducted with a simulated liquid nuclear waste containing high concentrations of complexing agents. The concentrations of actinides was equal to 8 x 10<sup>-8</sup> M for <sup>233</sup>U(VI) and 3 x 10<sup>-9</sup> M for <sup>239</sup>Pu(IV). Sorbent concentrations were 0.5 g L<sup>-1</sup> of GO, commercial bentonite

(SC “Khakassiyabentonite”, Russia) and granular activated carbon (Sigma-Aldrich). For HRTEM, GO aggregates were deposited onto a carbon-coated TEM grid and analyzed using HRTEM (JEOL-2100F) at an accelerating voltage of 200 kV. EDX analysis was performed with a JED-2300 analyzer. The CCC was determined by addition of aliquots of solutions with cations, i.e. Na<sup>+</sup>, Ca<sup>2+</sup> and Eu<sup>3+</sup>, to GO suspension.

After the addition of the certain portion of solution that led to CCC, GO precipitated and was observed by the unaided eye after 1 h of equilibration [15].

**Preparation of Sorption Materials:** The graphite was exfoliated with the effect of high intensity ultrasound and delaminated graphene nanosheets were used for graphene oxide [16] preparations by improved Hummers method [17]. H<sub>2</sub>SO<sub>4</sub> (60 ml), H<sub>3</sub>PO<sub>4</sub> (10 ml), graphene (1 g) and KMnO<sub>4</sub> (3 g) were mixed in a round-bottom flask. The mixture was then heated to 40 °C and stirred for 6 h, affording a pink, dense suspension. The suspension was then poured onto a mixture of ice and 30% H<sub>2</sub>O<sub>2</sub> (200 ml) and the pink suspension quickly turned bright yellow.

The product was purified by dialysis (Spectra/Por 3 dialysis membrane) and centrifuged. Purified GO product was obtained as a brown, honey-like suspension. The oxidation was quantitative when the theoretical yield was assumed to equal the starting graphite mass. The elemental analysis of prepared GO showed an overall composition of C 48.8%, H 2.1% and O 49.1% (impurities from natural graphite: SiO<sub>2</sub> 1%, K<sub>2</sub>O<sub>3</sub> 2%, CaO 0.6%, TiO<sub>2</sub> 1.3%, CuO 1.5%, ZnO 1.5%). The content of carboxylic group -COOH in the graphene oxide was increased by reaction with monochloroacetic acid [18].

Graphene oxide polystyrene composite was synthesized using direct emulsion polymerization of styrene in the presence of graphene oxide at 90 °C [19]. Hydrothermal conditions were maintained in stainless steel stirred autoclave. The graphene oxide was dispersed in 400 ml distilled water. After that argon gas was used for 10 minutes to purge oxygen from the solution. Styrene (30 ml) and divinylbenzene (1 ml) were added into solution. The solution was under constant stirring and heating until the reaction temperature reached to 91 °C, after that 12 ml solution of sodium 4-styrenesulfonate (4.00 g of sodium 4-styrenesulfonate in 100.0 ml water) was added. After 3 min the 24 ml solution of sodium 4-styrenesulfonate (4.00 g of sodium 4-styrenesulfonate in 100.0 ml water) and 1 ml of the solution of potassium persulfate and sodium bicarbonate (1 g K<sub>2</sub>S<sub>2</sub>O<sub>8</sub> and 3.5 g NaHCO<sub>3</sub> in 100 ml water) was added. The reaction mixture is continuously stirred and heated. After 85 min a mixture of 6 ml styrene, 0.15 ml divinylbenzene, 24 ml of water, 24 ml solution of sodium 4-styrenesulfonate and 3 ml of the solution of potassium persulfate and sodium bicarbonate were added; heating and stirring continuous next hour. The obtained sample was centrifuged 10 minutes at 10 000 rpm. The main fraction was filtered off and dried at 60 °C.

**Sorption Experiments:** The sorption properties of produced nanomaterials were evaluated by batch sorption

experiments, based on the contact of solid material with tracer solution. The volume of the solution was 1.5 ml and the mass of the sorbent was 0.01 g. The salts CsCl and SrCl<sub>2</sub> were used as carrier for radionuclides <sup>137</sup>Cs and <sup>85</sup>Sr, respectively. In the case of the kinetics experiments the concentration of CsCl or SrCl<sub>2</sub> was 2\*10<sup>-6</sup> mol/L.

These solutions were spiked by <sup>137</sup>Cs or <sup>85</sup>Sr. The contact time was 24 hours unless otherwise specified.

Sorption experiments were carried out at 24°C under atmospheric conditions. After the adsorption of radionuclides, the suspension was filtered and an aliquot of the supernatant was measured on the gamma spectrometer (EMPOS MC1256) using NaI(Tl) detector. The volume of measured aliquot was 0.5 ml.

The sorption experiments were described by the distribution coefficient (*K<sub>d</sub>*) and percentage of the sorption. The definition of *K<sub>d</sub>* is following:

$$K_d = \frac{c_{\text{mass}}}{c_{\text{volume}}} \cdot \frac{V}{m} [\text{ml/g}], \quad (1)$$

Where *c<sub>mass</sub>* is the concentration of the sorbate adsorbed onto the solid phase, *c<sub>volume</sub>* is the concentration of the sorbate in solution, *V* [ml] is the volume of the liquid phase and *m* [g] is the mass of the sorbent.

Langmuir (2) and Freundlich isotherm (3) were utilized for evaluation of the sorption data. The cation exchange capacity was determined by Langmuir isotherm:

$$q_e = \frac{KLq_{\text{max}}c_e}{1+KLc_e} [\text{mg/g}], \quad (2)$$

Where *q<sub>max</sub>* is the maximum sorbate uptake (mg/g), *KL* is the coefficient (L/mol), *c<sub>e</sub>* is the equilibrium concentration of the solute (mg/L) and *q<sub>e</sub>* is the adsorbed amount of the sorbate on the sorbent (mg/g).

Freundlich isotherm is defined as

$$q_e = K_F \cdot c_e^{1/n} [\text{mg/g}], \quad (3)$$

Where *K<sub>F</sub>* ((mg/g)/(mg/L)<sup>1/n</sup>) and *n* are characteristic constants related to the adsorption capacity and the adsorption intensity, respectively. The experimental data were fitted in program SciDAVis 0.2.4 that uses the nonlinear least-squares Marquardt-Levenberg algorithm for fitting.

## RESULTS AND DISCUSSIONS

Sorption kinetics and pH dependences are an important characteristic of the toxic element removal. Their reaction kinetics of with GO. Data on the sorption kinetics have indicated fast adsorption of all elements. The amount of adsorbed Co<sup>2+</sup>, Cu<sup>2+</sup>, Pb<sup>2+</sup> and Ni<sup>2+</sup> after 5 min varied from 70 to 90%. The equilibrium at 90–100% level was observed after 10–60 min of contact time. The pH of liquid-phase decreased from 5.4 ± 0.1 to 3.3 ± 0.1. Kinetic data were fitted to the pseudo-first-order kinetic model: *qt* = *q<sub>e</sub>* (1 - e<sup>-k<sub>ad</sub>t</sup>), where *qt* and *q<sub>e</sub>* are the studied element concentrations (μ mol g<sup>-1</sup>) at time *t* and equilibrium, respectively, while *k<sub>ad</sub>* (min<sup>-1</sup>) is the pseudo-first-order rate constant. The kinetic parameters showed that obtained data well fitted the pseudo-first-order equation.

The rate constants ranged from 0.29 to 0.46 min<sup>-1</sup> and increased in the following order: Co, Cu, Pb and Ni. Speciation of metals was not investigated during this study while it was reported that under close and identical conditions in the pH range from 3 to 5.4 the studied elements could exist as cations Co<sup>2+</sup>, Cu<sup>2+</sup>, Pb<sup>2+</sup> and Ni<sup>2+</sup> in the contact solutions [20-23]. Thus, we believe that pH-dependent species of elements could not affect the sorption kinetics. However, the sorption kinetic data followed well the electronegativity of elements (according to Allen's scale)—the rise of rate constants corresponds to the increase in electronegativity.

Studies of pH dependences indicated that about 100% of Ni was sorbed to GO at the initial pH of 3 to 8 after 24 h of contact time. Adsorption of Co gradually increased from 80 to 100%, while the amount of adsorbed Cu and Pb was decreased at pH of 7 and 8. For all elements the maximum adsorption was observed at initial pH values of 5 and 6. The pH values remained stable for 24 h in sorption experiments with MGO and Cu or Co at initial pH = 5.4 ± 0.1. Our preliminary data have indicated the maximum adsorption capacity of GO for Pb, Ni, Co and Cu of 573, 264, 253, 285 mg g<sup>-1</sup>, respectively, while the adsorption capacity of MGO for the studied elements was found to be 567, 127, 30, 133 mg g<sup>-1</sup>, respectively. The published data revealed wide variations of reported values, e.g. [Wu *et al*] showed that GO can possess a much higher adsorption capacity of 117.5 mg g<sup>-1</sup> for Cu(II) than that of activated carbon [20-24]. It has been demonstrated that GO had a high adsorption capability up to 1119 mg g<sup>-1</sup> toward Pb(II) ions in aqueous solutions [25, 26]. It was pointed out that the adsorption capacity of

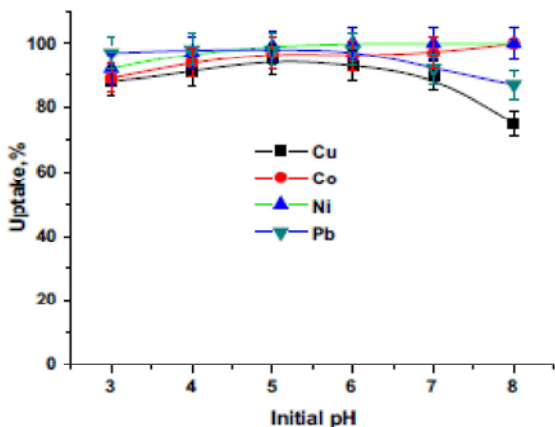


Fig. 2: Sorption of Cu, Co, Ni, Pb to GO depending on initial pH,  $C(\text{Cu, Co, Ni, Pb}) = 100 \text{ } \mu\text{mol L}^{-1}$ , contact time 24 h

GO was much higher as compared to the reported sorbents including nanomaterials e.g., carbon nanotubes [26]. Impressive adsorption capacities have been reported for the GO composites, e.g., sorption capacity of GO decorated with  $\text{Fe}_3\text{O}_4$ , sorption capacity of sulfonated magnetic GO composite and magnetic Mn-doped Fe(III) oxide nanoparticle implanted graphene for Cu(II) varied from 18.3 to 129.7  $\text{mg g}^{-1}$ , while for Pb(II) it ranged from 274.7 to 673  $\text{mg g}^{-1}$  [26-30]. They reported that the maximum adsorption capacity at pH of 7 of magnetic GO composite for Cu(II) was 59.44  $\text{mg g}^{-1}$  and for Pb(II) was 151.17  $\text{mg g}^{-1}$  were lower than that obtained in this study. Thus, the synthesized sorbents showed a similar or higher adsorption capacity as compared to the values reported in the recent publications with the exception of the GO adsorption capacity for Pb. The GO adsorption capacity of [than 1 g per g reported in previous publications for Pb was not reached in this study. Nevertheless, much higher adsorption capacities of all studied elements were found in sorption experiments with MGO which is important from the practical point of view.

**Radionuclide Interaction with GO:** The kinetics of radionuclide removal at pH ~3.5 by GO are represented, indicating that steady state conditions were achieved within 5 min even at very low GO concentration ( $<0.1 \text{ g L}^{-1}$  by carbon). The fast sorption kinetics are likely due to GO's highly accessible surface area [10,22] and its lack of internal surfaces that usually contribute to the slow kinetics of diffusion in cation-sorbent interaction. The fast kinetics are important for practical applications of GO for

removal of cationic impurities including  $\text{Th}_{(\text{IV})}$ ,  $\text{U}_{(\text{VI})}$ ,  $\text{Pu}_{(\text{IV})}$  and  $\text{Am}_{(\text{III})}$ . Fig. 3B and C show pH sorption edges for  $\text{Th}_{(\text{IV})}$ ,  $\text{Pu}_{(\text{IV})}$ ,  $\text{Am}_{(\text{III})}$ ,  $\text{Eu}_{(\text{III})}$ ,  $\text{U}_{(\text{VI})}$ ,  $\text{Sr}_{(\text{II})}$ ,  $\text{Tc}_{(\text{VII})}$  and  $\text{Np}_{(\text{V})}$ . All of the radionuclides demonstrate typical S-shaped pH-edges for cations, except for Tc, that exists as the pertechnetate anion. This explains its higher sorption at low pH when the GO surface is protonated and positively charged. Sorption of most of the cations is quantitative over a broad pH range; for  $\text{Th}_{(\text{IV})}$  and  $\text{Pu}_{(\text{IV})}$  complete sorption is achieved at  $\text{pH} > 1.5$  and for  $\text{Am}_{(\text{III})}$  and  $\text{Eu}_{(\text{III})}$  complete sorption occurs at  $\text{pH} > 2.3$ .

This suggests that GO would be useful in the remediation of contaminated natural waters. The position of the pH sorption edge is correlated to the formal cation charge. The sorption of U(VI) decreases at high pH ( $>7$ ), possibly due to  $\text{U}_{(\text{VI})}$  carbonate complexation. This was demonstrated earlier for mineral sorbents [23,24]. Further experiments demonstrated that the reversibility of sorption for Pu(IV) and U(VI) was quantitative.

When the pH was decreased, a new steady state was achieved in  $<10$  min, as shown in the inset.

GO has a high sorption capacity towards  $\text{U}_{(\text{VI})}$ ,  $\text{Sr}_{(\text{II})}$ ,  $\text{Am}_{(\text{III})}$  and  $\text{Eu}_{(\text{III})}$  cations as determined from the sorption isotherms shown in Fig. 3. Even at a GO concentration as low as  $0.038 \text{ g L}^{-1}$ , the saturation limit is not reached. The Langmuir sorption formalism (Equ 1) is:

$$C_{\text{sorb}} = \frac{Q_{\text{max}} K_L C_{\text{sol}}}{1 + K_L C_{\text{sol}}} \quad (1)$$

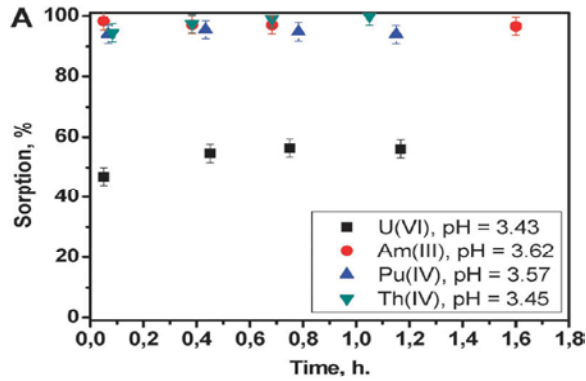
and the Freundlich sorption formalism (Equ 2) is:

$$C_{\text{sorb}} = K_F C_{\text{sol}}^n \quad (2)$$

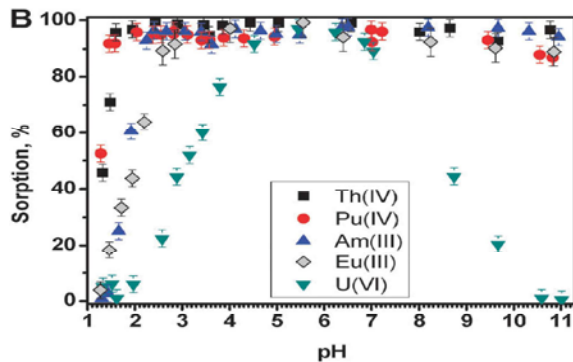
where  $C_{\text{sorb}}$  is the equilibrium concentration of radionuclides adsorbed on GO,  $C_{\text{sol}}$  is the equilibrium concentration of radionuclides in aqueous solution,  $Q_{\text{max}}$  is the maximum sorption capacity,  $K_L$  is a constant representing the strength with which the solute is bound to the substrate and  $K_F$  and  $n$  are empirical coefficients. In several cases the use of the Langmuir formalism (Equ 1) does not give as good a fit for the isotherm description as the Freundlich formalism (Equ 2). This is the case for  $\text{Am}_{(\text{III})}$ , for which sorption saturation is not reached under the experimental conditions. The values of the parameters for the Langmuir and Freundlich formalisms that are presented in Table 1 were calculated from experimental data, though the GO surface is far from saturation.

Table 1: Sorption of Cs and Sr on polystyrene and GO-polystyrene.

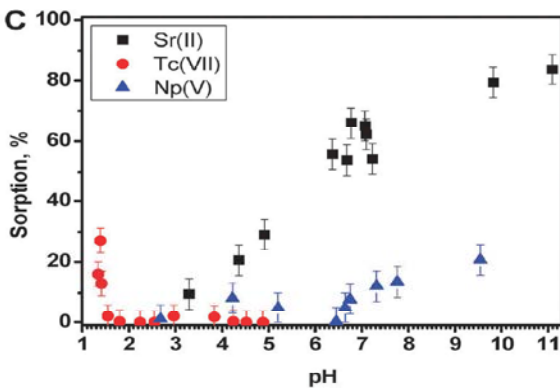
	Cs(I)		Sr(II)	
	%(Cs)	pH	%(Sr)	pH
Polystyrene	5	3.4	16.6	3.2
GO-polystyrene	90.2	4.8	98.4	5.3



(A) Kinetics of U(VI), Am(III), Th(IV) and Pu(IV) sorption onto GO indicating that steady state conditions are reached within 5 min.



(B) pH-sorption edges for Th(IV), U(VI), Pu(IV), Eu(III) and Am(III).



(C) pH-sorption edges for Sr(II), c(VII), Np(V) at steady state. The concentrations are listed in the Experimental section.

Fig. 3: Radionuclides removal by GO.

Data presented in Table 1 demonstrated that the sorption of Cs(I) and Sr(II) on polystyrene (it was prepared by the same method like the composite material only without adding of GO) and on the composite material GO-polystyrene. The results demonstrated that sorption of selected radionuclides is on the pure polystyrene very low - only 5.0 % for Cs(I) and 16.6 % for Sr(II). On the other side, the sorption on GO-polystyrene is very high - 90,2 % for Cs(I) and 98,4 % for Sr(II). Therefore the modification of polystyrene by GO increases the sorption properties.

Figure 4 demonstrated that the sorption kinetics of GO-polystyrene is very fast for both radionuclides. The Cs(I) reach maximum after 2 hours, the Sr(II) reach maximum after 1 hour. The pH of equilibrium solution for Cs(I) was around 5.0 and for Sr(II) pH was around 5.5.

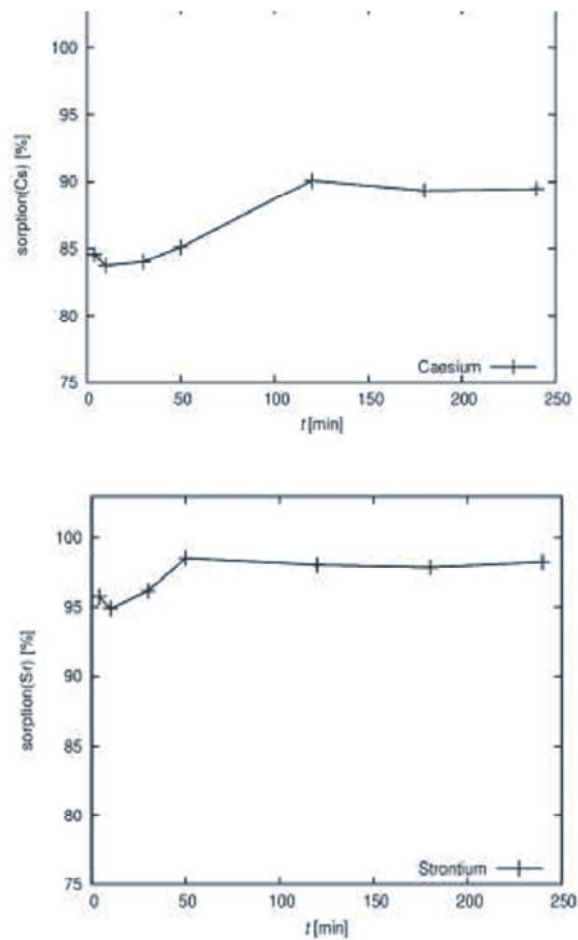


Fig. 4: Dependence of the sorption of Cs(I) (left) and Sr(II) (right) on contact time; V = 1.5 ml; m = 0.01 g; temperature 24 °C.

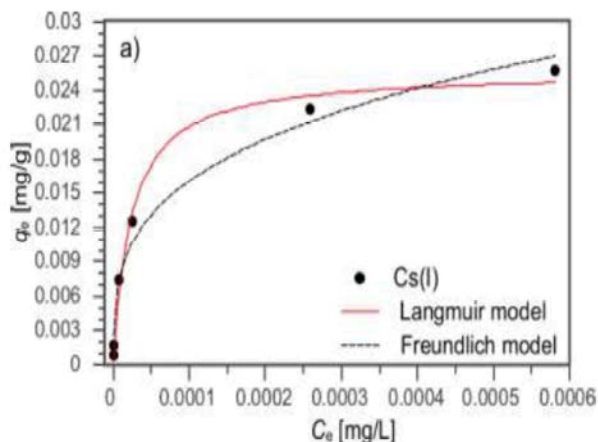


Fig. 5: Experimental data and Langmuir and Freundlich isotherms of Cs(I);  $V = 1.5$  ml;  $m = 0.01$  g; temperature  $24$  °C.

Table 2: Parameters for Langmuir and Freundlich models of Cs(I) adsorption on GO-polystyrene at temperature  $24$  °C.

Langmuir model			Freundlich model		
$Q_{max}$ [mg/g]	$KL$ [L/mol]	$R_2$	$KF$ [(mg/g)/(mg/L) <sup>1/n</sup> ]	$n$	$R_2$
0,026	43032	0,990	0,243	3,39	0,977

Fig. 5 demonstrated that the experimental data and Langmuir and Freundlich isotherms of Cs(I). Also data presented in Table 2 demonstrated that the parameters of Langmuir and Freundlich models of Cs(I) adsorption on GO-polystyrene. As can be seen in Table 2, the adsorption of Cs(I) on GO-polystyrene can be better fitted by Langmuir model ( $R_2 = 0.990$ ) compared to Freundlich model ( $R_2 = 0.977$ ). The maximum adsorption capacities ( $q_{max}$ ) of GO-polystyrene calculated from Langmuir model at pH 4.0 and temperature  $24$  °C were  $0.026$  mg/g for Cs(I).

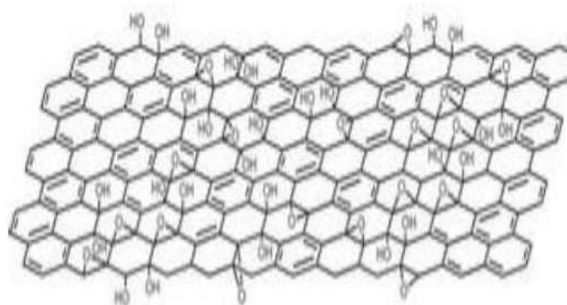
**How Graphene Oxide Works:** The amphiphilic GO produces stable suspensions when dispersed in liquids and shows excellent sorption capacities. Previously it was shown that GO enables effective removal of Cu, Co and Cd, Eu, arsenate and organic solvents. The surface of GO is functionalized with epoxy, hydroxyl and carboxyl moieties; the formation and composition of GO has been extensively studied. The surface moieties are well-suited for interaction with cations and anions.

The fast sorption kinetics are likely due to GO's highly accessible surface area and its lack of internal surfaces that usually contribute to the slow kinetics of diffusion in cation-sorbent interaction. The fast kinetics are important for practical applications of GO for removal of cationic impurities. GO has a high sorption capacity towards U, Sr, Am and Eucations as determined from the

sorption isotherms. Even at a GO concentration as low as  $0.038$  g/L, the saturation limit is not reached.

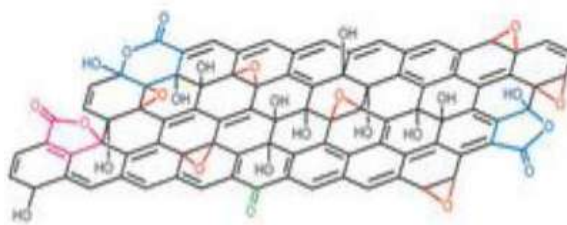
Low-valence ions such as calcium and iron also adsorb onto GO's surface, but, unlike high-valence ions, they don't destabilize the suspension. That itself leads to the formation of stable complexes, completely immobilizing the cations. Thus for low-valence ions, adsorption is reversible and insignificant. Conveniently, anions such as chloride and carbonate, being negatively charged, are not attracted by GO, so neither of these species interferes with radionuclide adsorption.

#### b) Lerf-Klinowski model



a) The chemical structure of a single sheet of Graphene Oxide according to the Lerf-Klinowski model [15, 16].

#### a) Updated chemical structure proposed by Gao and colleagues



b) An updated chemical structure proposed by Gao and colleagues [17].

Fig. 6: Explain how graphene oxide works

The selectivity of heavy radioactive ion absorption by GO against lighter ions, the ones that yield water salinity, not only allows more effective concentration of radioactive materials into solids, the volume of which is the only price-determining factor in the radionuclide recycling process, but also allows their use in non-desalinated water, where many other sorbents fail.



## CONCLUSION

This research hopes to find a less expensive and easier way of cleaning up radioactive accidents and leaks by demonstrating an ability of the GO to effectively and efficiently filter radionuclides from water sources such as rain water runoff or holding tank water.

GO demonstrated high sorption affinity towards the most toxic radionuclides from various solutions. GO is found to be much more effective when compared to bentonite clays or activated carbon in actinide removal from liquid nuclear wastes. The GO-containing radionuclide could be easily coagulated and precipitated. The simplicity of industrial scale-up of GO, its high sorption capacity and its ability to coagulate with cations makes it a promising new material for responsible radionuclide containment and removal. Nanocomposite material GO-polystyrene have been successfully prepared by the direct emulsion polymerization of styrene in the presence of GO. The results (Table 1) demonstrate that GO-polystyrene has enhanced sorption properties for Cs(I) and Sr(II) than polystyrene alone. The SEM demonstrates the morphology of GO-polystyrene – spherical polystyrene particles with diameter of 100-200 nm covered by GO. The Langmuir isotherm better fit experimental data than Freundlich isotherm as illustrated in Fig. 3. The maximum sorption capacity of Cs(I) was determined from Langmuir isotherm – 0,026 mg/g.

The obtained data on the sorption kinetics have indicated fast adsorption of  $\text{CO}^{2+}$ ,  $\text{Cu}^{2+}$ ,  $\text{Pb}^{2+}$  and  $\text{Ni}^{2+}$  after 5 min.

The equilibrium at the 90–100% level was reached after 10–60 min of contact time. The kinetic studies have shown that obtained data well fitted the pseudo-first-order equation.

Results obtained in this study have indicated that a higher level of GO oxidation can provide a higher magnetite loading and ensure insignificant pH variations and better sorption parameters for MGO. High variations in the uptake of studied elements depending on the pH require additional studies of sorption mechanisms.

## REFERENCES

1. Veerrier, D., J.A. Curtis and M.I. Greenberg, 2009. Clin Toxicol (Phila). May; 47(5): 393-406. doi: 10.1080/15563650902997849. Review.
2. Romanchuk Ayu, A.S. Slesarev, StN Kalmykov, D.V. Kosynkin and J.M. Tour, 2013. Graphene oxide for effective radionuclide removal. Phys. Chem. Chem. Phys., 15: 2321-2327.
3. National Research Council, Ground Water and Soil Cleanup, National Academy Press, Washington, D.C., 1999.
4. Special Fukushima Review session. Goldschmidt 2011 Earth, Life and Fire, Prague, Czech Republic, August 14–19 (abstract published in Mineral Magazine 2011, 75(3)).
5. Novoselov, K.S., A.K. Geim, S.V. Morozov, D. Jiang, Y. Zhang, S.V. Dubonos, I.V. Grigorieva and A.A. Firsov, 2004. Electric field effect in atomically thin carbon films. Science, 306: 666–669.
6. Mauter, M.S. and M. Elimelech, 2008. Environmental applications of carbon-based nanomaterials. Environ. Sci. Technol., 42(16): 5843-5859.
7. Zhu, Y., S. Murali, W. Cai, X. Li, J.W. Suk, J.R. Potts and R.S. Ruoff, 2010. Graphene and graphene oxide: synthesis, properties and applications. Adv Mater, 20: 1-19.
8. Ivanovskii, A.L., 2012. Graphene-based and graphene-like materials. Russ. Chem. Rev., 81:571-605.
9. Joshua Paul Concklin, May 2014, Radioactive Element Removal from Water Using Graphene Oxide (GO), An Undergraduate Research Scholars Thesis.
10. Kosynkin, D.V., G. Ceriotti, K.C. Wilson, J.R. Lomeda, J.T. Scorsone, A.D. Patel, J.E. Friedheim and J.M. Tour, 2012. ACS Appl. Mater. Interfaces, 4: 222-227.
11. Behabtu, N., J.R. Lomeda, M.J. Green, A.L. Higginbotham, A. Sinitiskii, D.V. Kosynkin, D. Tsentlovich, A.N.G. Parra Vasquez, J. Schmidt, E. Kesselman, *et al.*, 2010. Nat. Nanotechnol., 5: 406-411.
12. Stankovich, S., D.A. Dikin, G.H.B. Dommett, K.M. Kohlhaas, E.J. Zimney, E.A. Stach, R.D. Piner, S.T. Nguyen and R.S. Ruoff, 200. Nature, 442: 282-286.
13. Marcano, D.C., D.V. Kosynkin, J.M. Berlin, A. Sinitiskii, Z. Sun, A. Slesarev, L.B. Alemany, W. Lu and J.M. Tour, 2010. ACS Nano, 4: 4806-4814.
14. Dimiev, A., D.V. Kosynkin, L.B. Alemany, P. Chaguine and J.M. Tour, 2012. J. Am. Chem. Soc., 134: 2815-2822.
15. Anna, Yu. Romanchuk, Alexander S. Slesarev, Stepan N. Kalmykov, Dmitry V. Kosynkin and James M. Tour, 2013. Graphene oxide for effective radionuclide removal.
16. Brynych Vojtich, Kolářová Markéta, Pospichová Jana, Tolasz Jakub, Štengl Václav, Oct 14th - 16th 2015, Brno, Czech Republic, EU, Nanocon 2015.
17. Hummers, W.S. and R.E. Offeman, 1958. Preparation of Graphitic Oxide, J. Am. Chem. Soc., 80(6): 1339-1339.

18. Štengl, V., S. Bakardjieva, M. Bakardjiev, B. Štíbr and M. Kormunda, 2014. Carborane functionalized graphene oxide, a precursor for conductive self-assembled monolayers, *Carbon N.Y.*, 67: 336-343.
19. Sunkara, H.B., J.M. Jethmalani and W.T. Ford, 1994. Synthesis of crosslinked poly (styrene-co-sodium styrenesulfonate) latexes, *J. Polym. Sci. Part A Polym. Chem.*, 32(8): 1431-1435.
20. Wu, W., Y. Yang, H. Zhou, T. Ye, Z. Huang, R. Liu and Y. Kuang, 2013. Highly efficient removal of Cu (II) from aqueous solution by using graphene oxide. *Water Air Soil Pol.*, 224: 1372-1378.
21. Wenbao Jis, W. and S. Lu, 2014. Few-layered graphene oxides as superior adsorbents for the removal of Pb(II) ions from aqueous solutions. *Korean J. Chem. Eng.*, 31(7): 1265-1270.
22. Xing, H.T., J.H. Chen, X. Sun, Y.H. Huang, Z.B. Su, S.R. Hu, W. Weng, S.X. Li, H.X. Guo, W.B. Wu, Y.S. He, F.M. Li and Y. Huang, 2015. NH<sub>2</sub>- rich polymer/graphene oxide use as a novel adsorbent for removal of Cu(II) from aqueous solution. *Chem. Eng. J.*, 263: 280-289.
23. Sheng, G., S. Yang, J. Sheng, D. Zhao and X. Wang, 2011. Influence of solution chemistry on the removal of Ni(II) from aqueous solution to titanate nanotubes. *Chem. Eng. J.*, 168: 178-182.
24. Sitko, R., E. Turek, B. Zawisza, E. Malicka, E. Talik, J. Heimann, A. Gagor, B. Feist and R. Wrzalik, 2013. Adsorption of divalent metal ions from aqueous solutions using graphene oxide. *Dalton Trans*, 42: 5682-5689.
25. Sun, Y., Q. Wang, C. Chen, X. Tan and X. Wang, 2012. Interaction between Eu(III) and graphene oxide nanosheets investigated by batch and extended X-ray absorption fine structure spectroscopy and by modeling techniques. *Environ Sci. Technol.*, 46: 6020-6027.
26. Li, J., S. Zhang and C. Chen, 2012. Removal of Cu(II) and fulvic acid by graphene oxide nanosheets decorated with Fe<sub>3</sub>O<sub>4</sub> nanoparticles. *ACS Appl Mat Interf*, 4(9): 4991-5000.
27. Hu, X.J., Y.G. Liu and H. Wang, 2013. Removal of Cu(II) ions from aqueous solution using sulfonated magnetic graphene oxide composite. *Sep Purif Technol.*, 108: 189-195.
28. Nandi, D., T. Basu, S. Debnath, A.K. Ghosh, A. De and U.C. Ghosh, 2013. Mechanistic insight for the sorption of Cd(II) and Cu(II) from aqueous solution on magnetic Mn-doped Fe(III) oxide nanoparticle implanted graphene. *J. ChemEng Data*, 58(10): 2809-2818.
29. Kumar, S., R.R. Nair, P.B. Pillai, S.N. Gupta, M.A.R. Iyengar and A.K. Sood, 2014. Grapheneoxide-MnFe<sub>2</sub>O<sub>4</sub> magnetic nanohybrids for efficient removal of lead and arsenic from water. *ACS Appl Mat Interf*, 6: 17426-17436.
30. Zhang, Y., L. Yan and W. Xu, 2014. Adsorption of Pb(II) and Hg(II) from aqueous solution using magnetic CoFe<sub>2</sub>O<sub>4</sub>-reduced graphene oxide. *J. MolLiq*, 191: 177-182.